Polar Oxides

Properties, Characterization, and Imaging

Edited by
R. Waser, U. Böttger, and S. Tiedke

WILEY-VCH Verlag GmbH & Co. KGaA

Polar Oxides

Properties, Characterization, and Imaging

Edited by
R. Waser, U. Böttger, and S. Tiedke

Polar Oxides

Properties, Characterization, and Imaging

Edited by
R. Waser, U. Böttger, and S. Tiedke

WILEY-VCH Verlag GmbH & Co. KGaA

Editors

Rainer Waser
Department IFF &
CNI – Center of Nanoelectronic Systems
for Information Technology
Research Center Jülich, Germany
and
Institut für Werkstoffe der Elektrotechnik
RWTH Aachen, Germany
e-mail: waser@iwe.rwth-aachen.de

Ulrich Böttger
Institut für Werkstoffe der Elektrotechnik
RWTH Aachen, Germany
e-mail: boettger@ iwe.rwth-aachen.de

Stephan Tiedke
aixACCT Systems GmbH, Aachen, Germany
e-mail: tiedke@aixacct.com

Cover Picture
The picture shows an X-ray diffraction reciprocal space mapping (XRD-RSM) measurement at the 204 diffraction of a PZT 52/48 thin film on a SRO-STO substrate. A tetragonal phase with 90° domains as well as a pseudocubic phase induced by the strain of the substrate are observed.

Library of Congress Card No.: applied for
British Library Cataloging-in-Publication Data:
A catalogue record for this book is available from the British Library

Bibliographic information published by
Die Deutsche Bibliothek
Die Deutsche Bibliothek lists this publication in the Deutsche Nationalbibliografie; detailed bibliographic data is available in the Internet at <http://dnb.ddb.de>.

Printed in the Federal Republic of Germany
Printed on acid-free paper

Composition Thomas Pössinger, Aachen
Printing betz-druck GmbH, Darmstadt
Bookbinding Litges & Dopf Buchbinderei GmbH, Heppenheim

ISBN 3-527-40532-1

Contents

Preface

Polar oxides haved received increasing attention in recent years - both from a fundamental perspective and from a novel applications viewpoint. There are three major trends which led to this emphasis. One trend concerns the scaling of the structure size (particles size, device feature sizes, etc.) into the sub 100-nm regime. Although size effects on the nanometer scale have long been investigated, there has been a trend in recent years to strengthen the utilization of these effects and to synthesize oxide ceramics in which the properties are dominated by size effects. This is true for bulk ceramics and thick films as well as for thin films. A second trend concerns the fact that advanced functional components are made of material systems rather than of discrete materials. Material integration issues play an increasingly important role driven by the interest in integrating functions of polar oxides into conventional semiconductor chips as well as for the evolution of multifunctional components and systems. A third trend concerns the role of theory and modeling. The materials and device design is more and more accompanied and guided by modeling, e. g. by thermodynamics, finite-element methods, and ab-initio calculations.

This book is specifically addressed to the properties of polar oxides as well as to their chacterization and imaging techniques. The dielectric, optic, piezoelectric, pyroelectric behavior of this class of materials is discussed. Emphasis is placed on novel methods in the field of electrical and optical investigations, scanning probe microcoscopy (SPM) techniques and advanced X-ray analysis. The book starts with tutorial reviews, and arrives at up-to-date results about polar oxides. Therefore, it not only stimulates and further motivates young scientists but is of considerable interest for the members of our community.

The publication of this book follows a Workshop on "Polar Oxides – Properties, Characterizing and Imaging" which was held in Capri, Italy, in June 2003. The chapters published here are up-dated and revised manuscripts of the contributions presented during the workshop. The workshop was organized in the framework of "POLECER – European Thematic Network on Polar Electroceramics" which is part of the "Growth European Community Program".

The realization of the book is based on the work of many people. First of all, we would like to thank the authors, who make the book possible by their excellent contributions and their engaged cooperation. In addition, we would like to thank all members of our group at the RWTH Aachen, especially Thomas Pössinger for the preparing of the entire layout, Dagmar Leisten for editing and preparing the figures, and Maria Garcia for the spelling and format check.

We hope that the book will stimulate interest among a large number of its readers and give some motivation for their future work.

Rainer Waser, Ulrich Böttger, and Stephan Tiedke
Aachen, October 2004

1 Dielectric Properties of Polar Oxides

Ulrich Böttger

Institut für Werkstoffe der Elektrotechnik, RWTH Aachen, Germany

Abstract

This chapter gives an introduction to the class of polar oxides. Basic principles about symmetry classification, dielectric and ferroelectric polarization, phase transitions as well as electrical and piezoelectric properties are included. Landau-Ginzburg-Devonshire theory and the soft mode concept for the phase transition from an unpolar to a polar phase are also topic of this chapter. Specially addressed are the most relevant ferroelectric materials as $BaTiO_3$, $Pb(Zr,Ti)O_3$ and $SrBi_2Ta_2O_9$, and how the microstructure, modificatitions or doping will influence their properties. Ferroelectric domains evoked by the reduction of the electric and elastic energy are decisive for the dielectric and piezoelectric properties and the switching behavior. These effects are discussed for bulk ceramics as well as for thin films.

1.1 Introduction

Among the 32 crystallographic point groups describing all crystalline systems, 11 are centrosymmetric and contain an inversion center. In that case polar properties become not possible because any polar vector may be inverted by an existing symmetry transformation. All other 21 point groups without an inversion center (except the point group *432*) can exhibit piezoelectricity which describes the coupling between mechanical and electrical energies in a material. An external mechanical stress X leads to a change in the electric polarization P or dielectric displacement D respectively or an external electric field E causes an elastic strain x. The relation is given by the piezoelectric coefficient d_{ijk} being a third rank tensor (see Tutorial "Piezoelectric Characterization"):

$$D_i = d_{ijk} X_{jk} \qquad x_{ij} = d_{ijk} E_k \tag{1.1}$$

There are 10 polar groups with a unique polar axis among the 21 point groups without an inversion center. This class of crystals may show a spontaneous polarization parallel to the polar axis. E.g. barium titanate (in its tetragonal phase) is such a material (see Figure 1.1). However in the cubic phase (perovskite structure), the central titanium atom serves as an inversion center - then spontaneous polarization is not possible. Only with the occurrence of a tetragonal deformation, where the positively charged barium and titanium ions are displaced with respect to the six negatively charged oxygen ions, a polar axis is formed in the direction of the tetragonal deformation, which marks the direction of the spontaneous polarization [1].

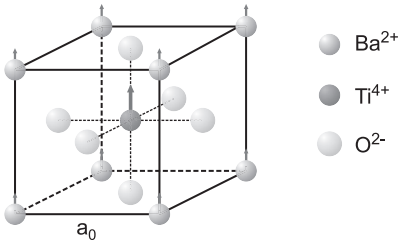

Figure 1.1: Unit cell of cubic $BaTiO_3$. The arrow schematically indicates one of the possible displacement of the central Ti^{4+} ion at the transition to the tetragonal ferroelectric structure that leads to a spontaneous polarization, in reality all ions are displaced against each other.

Following Maxwell's equations, the spontaneous polarization is connected with surface charges $P_s = \sigma$. The surface charges in general are compensated by charged defects. A temperature change changes the spontaneous polarization. This effect is called the pyroelectric effect.

If it is possible to reorient the spontaneous polarization of a material between crystallographically equivalent configurations by an external electric field, then in analogy to ferromagnetics one speaks about ferroelectrics. Thus, it is not the existence of spontaneous polarization alone, but the "switchability" by an external field which defines a ferroelectric material. Figure 1.2 displays a characteristic hysteresis loop occurring during the reversal of the polarization in a ferroelectric.

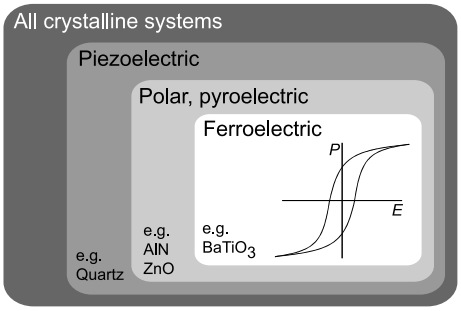

Figure 1.2: Classification of the crystallographic groups by their electrical properties

The class of ferroelectric materials have a lot of useful properties. High dielectric coefficients over a wide temperature and frequency range are used as dielectrics in integrated or in SMD (surface mounted device) capacitors. The large piezoelectric effect is applied in a variety of electromechanical sensors, actuators and transducers. Infrared sensors need a high pyroelectric coefficient which is available with this class of materials. Tunable thermistor properties in semiconducting ferroelectrics are used in PTCR (positive temperature coefficient

resistors). The significant non-linearities in electromechanical behavior, field tunable permittivities and refractive indices, and electrostrictive effects open up a broad field of further different applications. In addition, there is growing interest in ferroelectric materials for memory applications, where the direction of the spontaneous polarization is used to store information digitally.

1.2 Dielectric polarization

1.2.1 Macroscopic and microscopic view

In accordance to the Poisson equation, the source of the dielectric displacement $\vec{D}$ is given by the density of free (conducting) charges ρ:

$$\mathrm{div}\vec{D} = \rho_{\mathrm{free}} \tag{1.2}$$

The overall charge neutrality of matter in an external field is described by:

$$\vec{D} = \epsilon_0 \vec{E} + \vec{P} \tag{1.3}$$

The vacuum contribution caused by the externally applied electric field is represented by the term $\epsilon_0 \vec{E}$, and the electrical polarization of the matter in the system is described by $\vec{P}$, e.g. [2]. This relation is independent of the nature of the polarization which could be pyroelectric polarization, by piezoelectric polarization or dielectric polarization (by an external electric field).

Considering a simple parallel plate capacitor filled with matter (see Figure 1.3), two cases have to be distinguished: (i) If the applied voltage is kept constant ($E = \mathrm{const}$, short circuit condition), additional free charges need to flow into the system to increase D according to Equation (1.2). If the charges on the plates are kept constant ($D = \mathrm{const}$, open circuit condition), the electric field E and, hence, the voltage between the plates will decrease according to Equation (1.3).

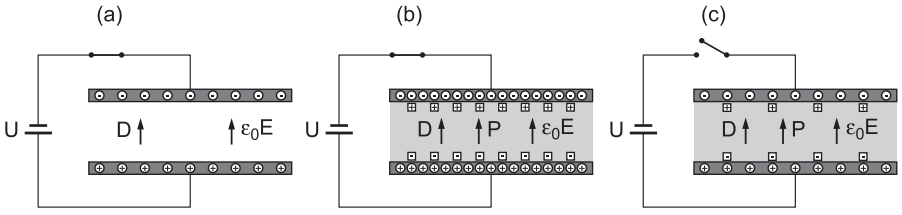

Figure 1.3: Parallel plate capacitor (a) without any dielectric, (b) filled with dielectric under short circuit condition ($E = \mathrm{constant}$) and (c) filled wtih dielectric under open circuit condition ($D = \mathrm{constant}$).

For a pure dielectric response of the matter the polarization is proportional to the electric field in a linear approximation by

$$P = \epsilon_0 \chi_e E \qquad \text{or} \qquad D = \epsilon_0 \epsilon_r E \tag{1.4}$$

The dielectric susceptibility χ is related to the relative dielectric constant ϵ_r by $\chi = \epsilon_r - 1$. Equations (1.4) are only valid for small fields. Large amplitudes of the ac field lead to strong non-linearities in dielectrics, and to sub-loops of the hysteresis in ferroelectrics. Furthermore, the dielectric response depends on the bias fields as shown in Figure 1.4. From the device point of view this effect achieves the potential of a tunable dielectric behavior, e. g. for varactors.

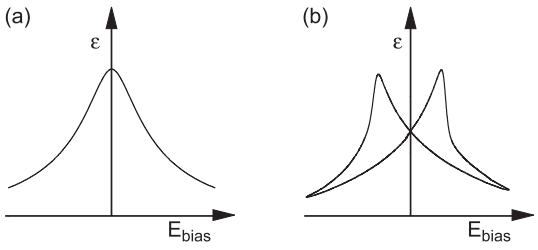

Figure 1.4: Bias field dependence of the dielectric constant of (a) dielectric and (b) ferroelectric material

Equations (1.3) and (1.4) describe the mean properties of the dielectric. This macroscopic point of view does not consider the microscopic origin of the polarization [3]. The macroscopic polarization P is the sum of all the individual dipole moments p_j of the material with the density N_j.

$$P = \sum_j N_j p_j \tag{1.5}$$

In order to find a correlation between the macroscopic polarization and the microscopic properties of the material a single (polarizable) particle is considered. A dipole moment is induced by the electric field at the position of the particle which is called the local electric field E_{loc}

$$p = \alpha E_{loc} \tag{1.6}$$

where α is the polarizability of an atomic dipole. If there is no interaction between the polarized particles, the local electric field is identical to the externally applied electric field $E_{loc} = E_0$, resulting in a simple relation between the susceptibility and the polarizability $\epsilon_0 \chi = N_j \alpha_j$.

In condensed matter, the density and therefore the electrostatic interaction between the microscopic dipoles is quite high. Hence, the local field E_{loc} at the position of a particular dipole is given by the superposition of the applied macroscopic field E_0 and the sum

of all other dipole fields. For cubic structures and for induced dipoles (ionic and electronic polarization), the calculation reveals a relation between the atomic polarizability α and the macroscopic permittivity $\epsilon = \epsilon_0 \epsilon_r$ which is referred to the Clausius-Mossotti equation [4].

$$\epsilon = \frac{\epsilon_0 + 2N_j\alpha_j}{\epsilon_0 - N_j\alpha_j} \tag{1.7}$$

1.2.2 Mechanisms of polarization

In general, there are five different mechanisms of polarization which can contribute to the dielectric response [3].

- **Electronic polarization** exists in all dielectrics. It is based on the displacement of the negatively charged electron shell against the positively charged core. The electronic polarizability α_{el} is approximately proportional to the volume of the electron shell. Thus, in general α_{el} is temperature-independent, and large atoms have a large electronic polarizability.

- **Ionic polarization** is observed in ionic crystals and describes the displacement of the positive and negative sublattices under an applied electric field.

- **Orientation polarization** describes the alignment of permanent dipoles. At ambient temperatures, usually all dipole moments have statistical distribution of their directions. An electric field generates a preferred direction for the dipoles, while the thermal movement of the atoms perturbs the alignment. The average degree of orientation is given by the Langevin function $\langle \alpha_{or} \rangle = p^2/(3k_BT)$ where k_B denotes the Boltzmann constant and T the absolute temperature.

- **Space charge polarization** could exist in dielectric materials which show spatial inhomogeneities of charge carrier densities. Space charge polarization effects are not only of importance in semiconductor field-effect devices, they also occur in ceramics with electrically conducting grains and insulating grain boundaries (so-called Maxwell-Wagner polarization).

- **Domain wall polarization** plays a decisive role in ferroelectric materials and contributes to the overall dielectric response. The motion of a domain wall that separates regions of different oriented polarization takes place by the fact that favored oriented domains with respect to the applied field tends to grow.

The total polarization of dielectric material results from all the contributions discussed above. The contributions from the lattice are called intrinsic contributions, in contrast to extrinsic contributions.

$$\epsilon = \underbrace{\epsilon_{elec} + \epsilon_{ion}}_{intrinsic} + \underbrace{\epsilon_{or} + \epsilon_{dw} + \epsilon_{sc}}_{extrinsic} \tag{1.8}$$

Each contribution stems from a short-range movement of charges that responds to an electric field on different time scales and, hence, through a Fourier transform, in different frequency

regimes. If the oscillating masses experience a restoring force, a relaxation behavior is found (for orientation, domain walls, and space charge polarization). Resonance effects are observed for the ionic and electronic polarization. The dispersion of the dielectric function is shown in Figure 1.5, and holds the potential to separate the different dielectric contributions.

The space charge polarization is caused by a drift of mobile ions or electrons which are confined to outer or inner interfaces. Depending on the local conductivity, the space charge polarization may occur over a wide frequency range from mHz up to MHz. The polarization due to the orientation of electric dipoles takes place in the frequency regime from mHz in the case of the reorientation of polar ligands of polymers up to a few GHz in liquids such as water. It is often possible to distinguish between space charge and orientation because of the temperature dependence of α_{or}. In the infrared region between 1 and 10 THz, resonances of the molecular vibrations and ionic lattices constituting the upper frequency limit of the ionic polarization are observed. The resonance of the electronic polarization is around 10^{15} Hz. It can be investigated by optical methods.

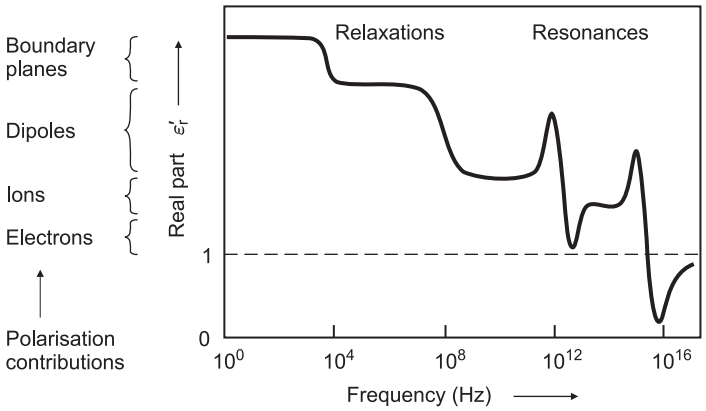

Figure 1.5: Frequency dependence of real part of the dielectric function.

The dispersion of the dielectric response of each contribution leads to dielectric losses of the matter which can be mathematically expressed by a complex dielectric permittivity:

$$\epsilon = \epsilon' + i\epsilon'' \tag{1.9}$$

Dielectric losses are usually described by the loss tangent:

$$\tan\delta = \frac{\epsilon''}{\epsilon'} \tag{1.10}$$

It should be taken into account that the general definition of the $\tan\delta$ is related to the ratio of loss energy and reactive energy (per periode), i. e. all measurements of the loss tangent also include possible contributions of conductivity σ of a non-ideal dielectric given by $\tan\delta = \sigma/\omega\epsilon'$.

1.3 Ferroelectric polarization

An ideal single crystal shows a $P(E)$ behavior as depicted in Figure 1.6. The non-ferroelectric dielectric ionic and electronic polarization contributions are clearly linear, and are suposed by the spontaneous polarization P_s (dashed curve in Figure 1.6). To reverse the polarization an electrical field with an amplitude $E > E_c$ is required. In opposite to single crystals in poly-domain ferroelectric ceramics, the remanent polarization P_r is smaller than the spontaneous one P_s due to backswitching even for opposite fields as shown in Figure 1.6. In that case P_s can be estimated by extrapolation of (non-switching) P-values to $E \to 0$.

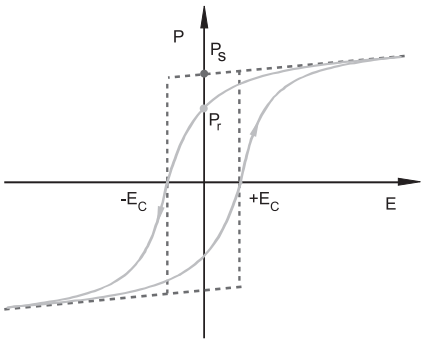

Figure 1.6: Ferroelectric hysteresis of single domain single crystal (dashed line) and polycrystalline sample (full line)

A ferroelectric "model" material is barium titanate $BaTiO_3$. On cooling from high temperatures, the permittivity increases up to values well above 10,000 at the phase transition temperature T_C. The inverse susceptibility as well as the dielectric permittivity follows a Curie-Weiss law $\chi^{-1} \approx \epsilon^{-1} \propto (T - \Theta)$. The appearance of the spontaneous polarization is accompanied with a spontaneous (tetragonal) lattice distortion.

The phase transition in barium titanate is of first order, and as a result, there is a discontinuity in the polarization, lattice constant, and many other properties, as becomes clear in Figure 1.7. It is also clear in the figure that there are three phase transitions in barium titanate having the following sequence upon cooling: rhombohedral, orthorhombic, tetragonal and cubic.

There is a small thermal hysteresis of the transition temperature, which depends on many parameters such as the rate of temperature change, mechanical stresses or crystal imperfections. From a crystal chemical view, the Ba-O framework evokes an interstitial for the central Ti^{4+} ion which is larger than the actual size of the Ti^{4+} ion. As a result, the serie of phase transformations takes place to reduce the Ti cavity size. Certainly, the radii of the ions involved impact the propensity for forming ferroelectric phases; thus both $PbTiO_3$ and $BaTiO_3$ have ferroelectric phases, while $CaTiO_3$ and $SrTiO_3$ do not [5].

The optical properties of ferroelectric materials are characterized by birefringence. Barium titanate is isotropic only in the cubic phase. The tetragonal and the rhombohedral phases are

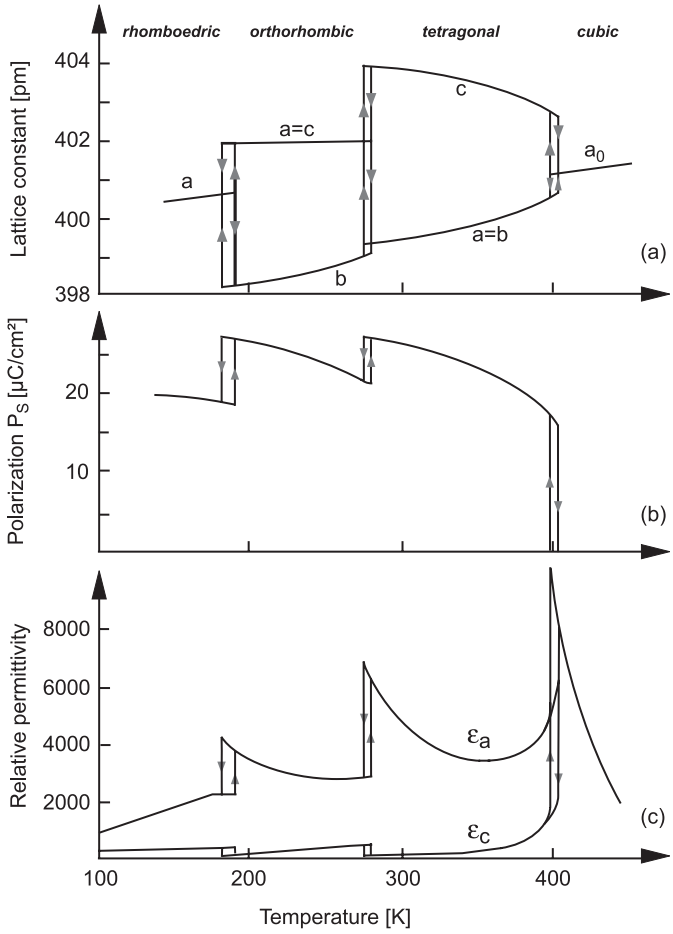

Figure 1.7: Various properties of barium titanate as a function of temperature. Anisotropic properties are shown with respect to the lattice direction. (a) Lattice constants, (b) spontaneous polarization P_s and (c) relative permittivity ϵ_r.

uniaxially birefringent while the orthorhombic phase exhibits birefringent behavior with two axes. Figure 1.7 (c) displays the temperature dependence of the permittivity in $BaTiO_3$.

1.4 Theory of Ferroelectric Phase Transition

1.4.1 Ginzburg-Landau Theory

The Ginzburg-Landau theory is equivalent to a mean field theory considering the thermodynamic entity of the dipoles in the mean field of all the others. It is reasonable if the particular

dipole interacts with many other dipoles. The theory introduces an order parameter P, i.e. the polarization, which for a second order phase transition diminishes continuously to zero at the phase transition temperature T_c [3]. Close to the phase transition, therefore, the free energy may be written as an expansion of powers of the order parameter. All the odd powers of P do not occur because of symmetry reasons.

$$F(P,T) = \frac{1}{2}g_2P^2 + \frac{1}{4}g_4P^4 + \frac{1}{6}g_6P^6 \tag{1.11}$$

The highest expansion coefficient (here g_6) needs to be larger than zero because otherwise the free energy would approach minus infinity for large P. All coefficients depend on the temperature and in particular the coefficient g_2. Expanding g_2 in a series of T around the Curie temperature Θ which is equal to or less than the phase transition temperature T_c, we can approximate:

$$g_2 = \frac{1}{C}(T - \Theta). \tag{1.12}$$

Stable states are characterized by minima of the free energy with the necessary and sufficient conditions:

$$\frac{\partial F}{\partial P} = P(g_2 + g_4P^2 + g_6P^4) = 0 \tag{1.13}$$

$$\text{and} \qquad \frac{\partial^2 F}{\partial P^2} = \frac{1}{\chi} = g_2 + 3g_4P + 5g_6P^3 > 0 \tag{1.14}$$

Two cases are to distinguish: (i) $g_4 > 0 \Rightarrow g_6 \approx 0$ which corresponds to a phase transition of second order, and (ii) $g_4 < 0 \Rightarrow g_6 > 0$ which is related with a phase transition of first order. In both cases, the trivial solution $P = 0$ exists, representing the paraelectric phase. Inserting Equation (1.12) into (1.14) it becomes obvious that above T_c the coefficient g_2 needs to be larger than zero in order to obtain stable solutions. A comparison of Equation (1.12) and (1.14) shows that g_2 is expressed by the susceptibility χ, for which a Curie-Weiss law is found.

$$\chi = \frac{C}{T - \Theta} \tag{1.15}$$

Second order phase transition

For $T < \Theta$ a spontaneous polarization exists. It can easily be shown that the Curie temperature Θ is equal to the phase transition temperature T_C. The spontaneous polarization depends on the distance from the phase transition temperature with a square root law.

$$P_s = \sqrt{\frac{T_c - T}{Cg_4}} \tag{1.16}$$

Figure 1.8 schematically displays the free energy close to the second order phase transition for different temperatures as a function of the order parameter P_s. For $T > T_c$ a minimum

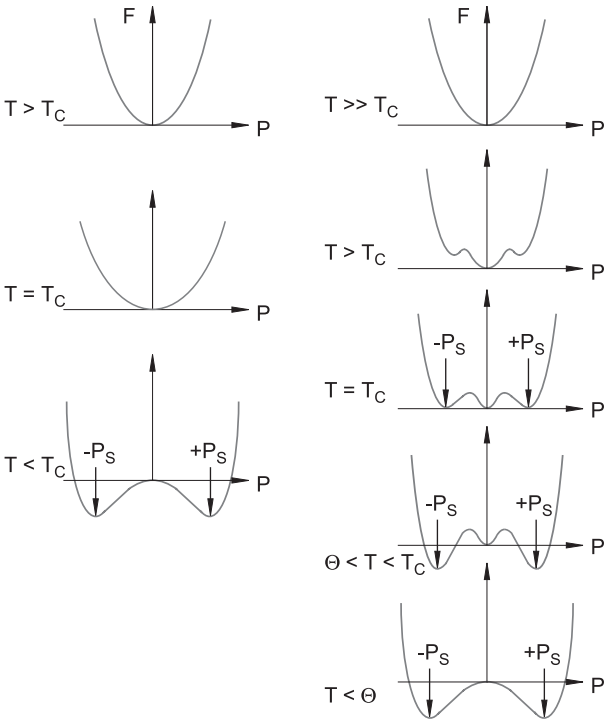

Figure 1.8: Free energy of a ferroelectric with a second-order phase transition (left) and with a first-order phase transition (right) at different temperatures. T_C is the phase transition temperature and Θ is the Curie temperature .

is found for $P^2 = 0$. At $T = T_c$, this minimum shifts continuously to final values of the polarization. The temperature dependence of the susceptibility in the ferroelectric phase is obtained by inserting Equation (1.16) into (1.14).

$$\left.\frac{1}{\chi}\right|_{T<T_c} = 2\,\frac{T_c - T}{C} \tag{1.17}$$

The slope of the inverse susceptibility below T_c is just twice of the slope above T_c. The theory is in good agreement to the experimental data, see Figure 1.9.

First order phase transition

If the expansion coefficients are chosen as $g_4 < 0$ and $g_6 > 0$, stable states will again be found from Equation (1.13):

$$P_s^2 = \frac{1}{2g_6}\left(|g_4| + \sqrt{g_4^2 - 4C^{-1}(T-\Theta)g_6}\right) \tag{1.18}$$

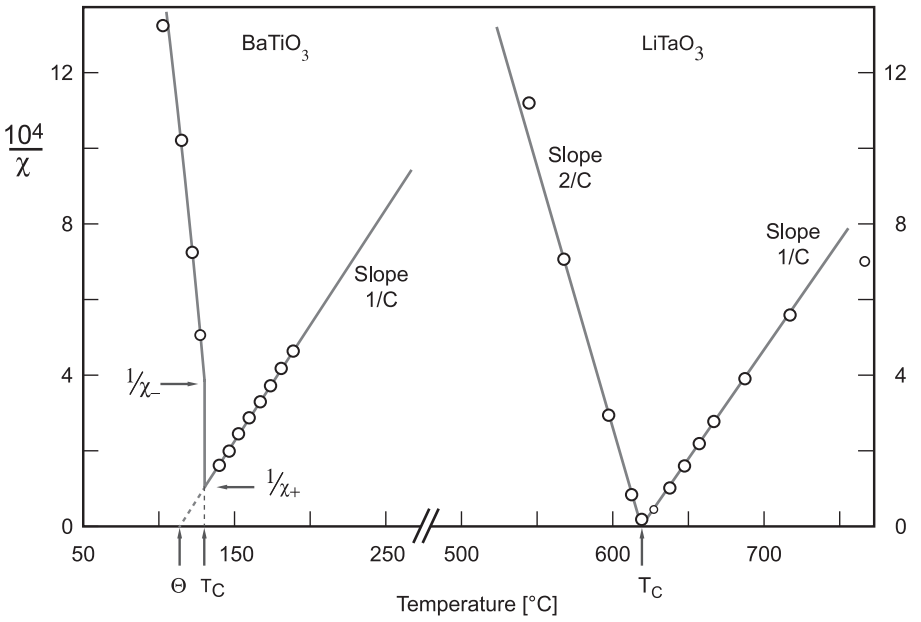

Figure 1.9: Reciprocal dielectric susceptibility at the phase transition of lithium tantalate (second order phase transition) and of barium titanate (first order phase transition).

Inserting Equation (1.18) into (1.11) results in the free energy as a function of polarization and of temperature. In Figure 1.8 the behavior of $F(P_s, T)$ is shown for some relevant temperatures. At high temperatures the free energy assumes a parabolic shape with a minimum corresponding to a stable paraelectric phase. During cooling, secondary minima at finite polarizations become visible. Their energy level at the beginning, however, is higher than that at $P = 0$. In this regime the paraelectric phase is stable and the ferroelectric phase metastable. Lowering the temperature further, at $T = T_C$ all three minima of the free energy are at the same level. Below T_C ,F becomes negative and favors a finite spontaneous polarization. In the temperature regime between T_C and Θ the paraelectric phase coexists with the ferroelectric phase with the paraelectric phase being metastable. Somewhere during cooling through this regime, the first order phase transition to the ferroelectric state will occur with a corresponding jump of the spontaneous polarization from zero to a finite value.

The susceptibility in the ferroelectric phase is given by:

$$\left.\frac{1}{\chi}\right|_{T<T_c} = \frac{3g_4^2}{4g_6} + 8\frac{T - T_c}{C} \tag{1.19}$$

The dielectric behavior closed to a phase transistion is displayed in Figure 1.9 for barium titanate (first-order transition with $T_c = 135°\text{C}$, $C = 1.8 \cdot 10^5\,°\text{C}$) and for lithium tantalate (second-order transition with $T_c = 618°\text{C}$ and $C = 1.6 \cdot 10^5\,°\text{C}$).

1.4.2 Soft Mode Concept

The atoms of a crystal vibrate around their equilibrium position at finite temperatures. There are lattice waves propagating with certain wavelengths and frequencies through the crystal [7]. The characteristic wave vector $\vec{q}$ can be reduced to the first Brillouin zone of the reciprocal lattice, $0 \leq q \leq \pi/a$, when a is the lattice constant.

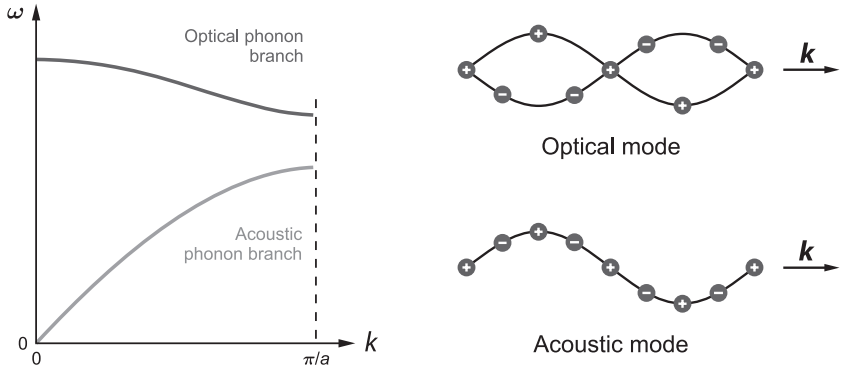

Figure 1.10: Transverse acoustic (TA) and optic mode (TO) of the phonon spectrum.

In every lattice there are three modes with different frequencies belonging to one longitudinal and two transverse branch of the acoustic phonons, as shown in Figure 1.10. A vibration of the atoms perpendicular to the propagation corresponds to a transverse wave, a vibration in the direction of the propagation corresponds to a longitudinal wave. The acoustic phonons have an elastic nature. All atoms vibrate as a linear chain independent of the number of different atoms per lattice cell. The wavelengths of the acoustic phonons are given by the sound velocity v_s, therefore, no coupling of acoustic phonons with electromagnetic waves exists ($v_s \ll v_{\mathrm{Light}}$).

In case of non-primitive lattices with different atoms in the elementary cell, the sub-lattices can vibrate against each other (optical modes, see Figure 1.10). A vibration with a frequency $\omega \neq 0$ becomes possible even for $k = 0$. The opposite movement of neighboring atoms evokes large dipole moments allowing a coupling to electromagnetic waves.

In general, each mode of the phonon dispersion spectra is collectively characterized by the relating energy, i.e. the frequency and wave vector k, and is associated with a specific distortion of the structure.

The local electric field in ionic crystals leads to a splitting of the optical vibration modes. The longitudinal mode frequency is shifted to higher frequencies while the transverse mode frequency is shifted to lower frequencies. The softening of the transverse modes is caused by a partial compensation of the short-range lattice (elastic) forces on the one hand and the long-range electric fields on the other hand. This effect is strongest at the zone center [3]. If the compensation is complete, the transverse optic mode frequency becomes zero when the temperature is decreased, $\omega_{\mathrm{TO}}(T \rightarrow T_c) \rightarrow 0$, and the soft phonon condenses out so that at

T_c a phase transition to a state with spontaneous polarization takes place (ferroelectric phase transition). The mechanism becomes clearer considering Figure 1.11 (b). At the zone center ($k = 0$) the wavelength of the TO mode is infinite ($\lambda \to \infty$), i.e the region of homogeneous polarization becomes infinite. In the case of the softening of the TO mode the transverse frequency becomes zero and no vibration exists anymore ("frozen in").

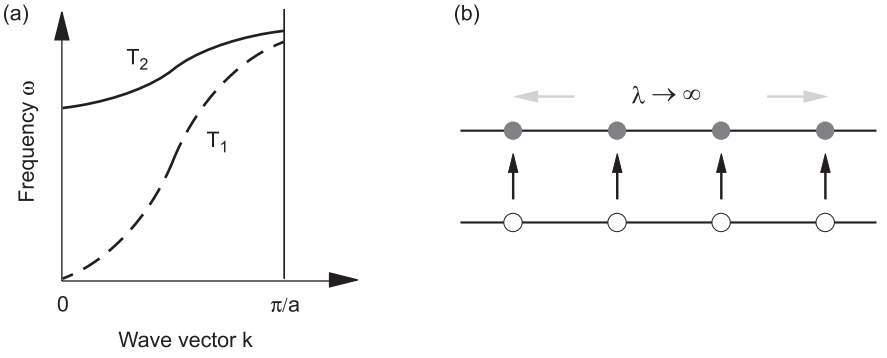

Figure 1.11: (a) Softening of the TO modes for $T_2 > T_1$ at the Brillouin zone center and (b) freezing of the TO modes for $T \to T_c$.

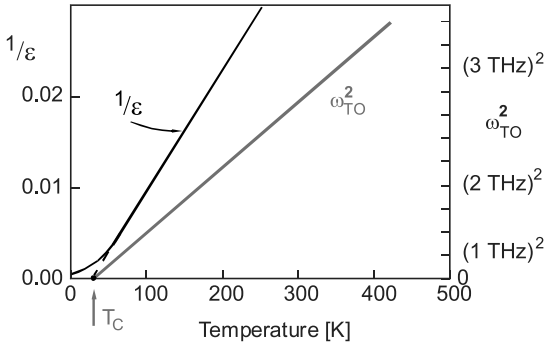

Figure 1.12: Frequency of the TO mode and dielectric behavior at the phase transition

A linear relation between ω_{TO}^2 and T at the zone center is found (see Figure 1.12) suggesting that the temperature dependence of the optic mode frequency relates to the phase transition. In accordance with the Lyddane-Sachs-Teller relation

$$\frac{\epsilon_s(T)}{\epsilon_\infty} = \frac{\omega_{\mathrm{LO}}^2}{\omega_{\mathrm{TO}}^2(T)} \tag{1.20}$$

ω_{TO} relates directly to the dielectric constant ϵ_s, i.e. the dielectric anomaly is associated with a soft mode condensation. From the extrapolation according to Equation (1.15) a phase transition at $T_c = 50$ K would be expected. This phase transition, however, does not really take place. It is dominated by a competing displacive phase transition at the zone boundary.

1.5 Ferroelectric Materials

1.5.1 Basic Compositions

Many ferroelectric materials were found in the past. However, there is a limited number of structures that are adopted by the majority of the commercially important ferroelectric materials. In each of these structures, the ferroelectricity is tied to distortion of the coordination polyhedra of one or more of the cations in the structure. One example is the perovskite structure. Cations that seem to be especially susceptible to forming such distorted polyhedra include Ti, Zr, Nb, Ta, and Hf. All of these ions lie near crossover points between the stability of different electronic orbitals, and so may be likely to form distorted coordination polyhedra [5]. Polarizable cations such as Pb and Bi are also common to many ferroelectric materials. In this case, it has been suggested that the lone pair electrons may play an important role in stabilizing ferroelectric structures. Thus the ferroelectric transition temperature and spontaneous distortion of $PbTiO_3$ is much larger than that of $BaTiO_3$.

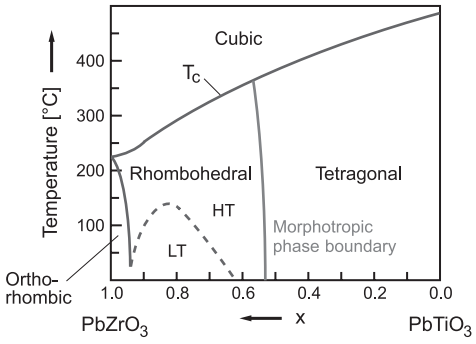

Figure 1.13: Phase diagram for PZT showing the morphotropic phase boundary between rhombohedral and tetragonal phases.

Solid solutions of $PbTiO_3$-$PbZrO_3$ (PZT) are one of the most important ferroelectric and piezoelectric materials [6]. Over the entire solid solution range, PZT adopts distorted versions of the perovskite structure, as shown in Figure 1.13. At the morphotropic phase boundary (MPB), the tetragonal phase and the rhombohedral phase co-exists leading to a higher polarizibility due to the presence of a larger number of possible polarization directions (6 from tetragonal phase, and 8 from the rhombohedral phase). Thus, the dielectric and piezoelectric properties show strong maxima near this composition. The high piezoelectric coefficients

(i.e. d_{33} values of 250 to 400 pC/N), coupled with a high transition temperature are the main reason that PZT ceramics are so widely used as piezoelectric sensors and actuators. The orthorhombic phase near the $PbZrO_3$ side of the PZT phase diagram corresponds to an antiferroelectric distortion of the perovskite structure, in which the polarization is cancelled on a unit cell level. For ferroelectric memory applications utilizing PZT, mostly Ti-rich compositions are used because of their large spontaneous polarization available, in accordance to Equation (1.16), and because the hysteresis loops of ferroelectric thin films are squarer for tetragonal than for rhombohedral compositions. This typically results in remanent polarizations in excess of 30 $\mu C/cm^2$. Today, low density memories based on PZT are in commercial production, and there is a good prospect for scaling to high densities.

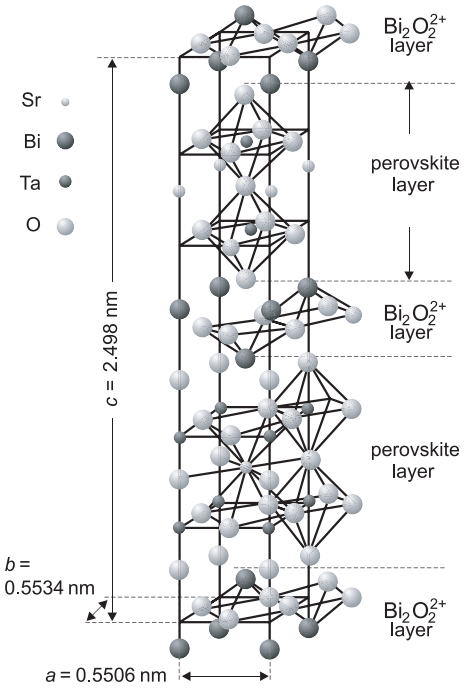

Figure 1.14: Bismuth layer structure SBT

An alternative structure that has also been widely investigated both for high temperature piezoelectric, as well as for ferroelectric memory applications is the bismuth layer structure family as shown in Figure 1.14 for $SrBi_2Ta_2O_9$ (SBT), e.g. [8]. The structure consists of perovskite layers of different thicknesses, separated by $Bi_2O_2^{2+}$ layers. It has been shown that when the perovskite block is an even number of octahedra thick, the symmetry imposes a restriction on the polarization direction, confining it to the a-b plane. In contrast, when the perovskite block is an odd number of octahedra thick, it is possible to develop a component of the polarization along the c axis (nearly perpendicular to the layers). This could be used in

order to enhance the remanent polarization of ferroelectric thin films for memory applications; since there are comparatively few allowed directions for the spontaneous polarization, the remanent polarization is rather small for many film orientations as shown in comparison to PZT. However, the SBT materials are less susceptible to fatigue (a reduction in switchable polarization on repeated cycling).

It is important to realize that thin films may differ in some substantial ways from bulk ceramics or single crystals of the same composition. One source of these differences is the substantial in-plane stresses that thin films are typically under, ranging from MPa to GPa [9]. Because many ferroelectric materials are also ferroelastic, imposed stresses can markedly affect the stability of the ferroelectric phase, as well as the ease with which polarization can be reoriented in some directions. The phase diagram becomes considerably complicated by the presence of a dissimilar substrate [10]. It is obvious that the material coefficients are drastically changed.

1.5.2 Grain Size effects

In bulk $BaTiO_3$ ceramics the grain size has a strong effect on the low frequency permittivity for grain sizes below approx. 10 μm as shown in Figure 1.15 (a). The permittivity is rising at decreasing grain sizes up to a maximum at $g_m \approx 0.7\mu$m [11]. The increase of ϵ could be caused by internal stresses because each grain is clamped by its surrounding neighbors or by the increase of the number of domain walls contributing to the dielectric constant. Below this size g_m, the permittivity sharply decreases again in conjunction with a reduction of the tetragonality and of the remanent polarization. The drop in permittivity may be interpreted by the effect of a low permittivity interfacial layer of 0.5 to 2 nm thickness at the grain boundaries. This layer shows no difference of the composition and crystal structure in comparison to the bulk and is believed to be of photonic nature.

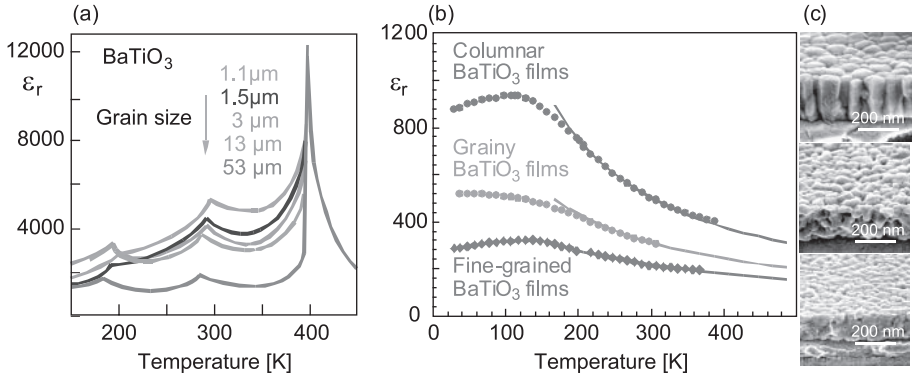

Figure 1.15: $BaTiO_3$: Temperature dependence of the permittivity for (a) bulk ceramics with different grain sizes and (b) thin films with different grain sizes and (c) microstructure of thin films.